UDC: 621.833.6(047)=20
COSATI: 20-11, 13-09, 14-02

Rade Kneževi , PhD (Eng)[1)]
Stanoje Cvetkovi , BSc (Mat)[1)]

Key words:

A general reason for chaotic and stochastic behaviour of dynamic systems is the loss of equilibrium stable position or motion, which is evident from the exponential dispersion of the neighbouring phase trajectories. However small excitations and disturbances might be, the representative point begins to "stray" from one closed curve to another and its position may become optional in time.

Chaotic and stochastic behaviour are caused by nonlinearity which, on its part, causes the homoclinic structure*. Homoclinic structure produces a mixture of unstableness, local diffusion and general cohering. *Stable periodic motion and equilibrium position may lose their stability or disappear in just a few particular cases* [1]:

- *Stable equilibrium position or periodic motion and a corresponding unstable motion blend together and disappear, creating a new stable position*.
- *Equilibrium state or periodic motion lose their stability, simultaneously creating a stable aperiodic motion or pass into corresponding two-dimensional torus multiplicities with periodic and quasi -periodic "coils" of phase trajectories.*
- *Stable periodic motion accumulates in one point passing into stable equilibrium or stillness, or it blends with the equilibrium creating bi-asymptotic curve as a cross section of its integral multiplicities.*
- *Periodic motion loses its stability and stable periodic motion of doubled period occurs simultaneously.*

The last transformation may recur indefinitely, forming an absolute series of doubled period bifurcation.

* Homoclinic structure – structure on a map, or transfer, developed during cutting in the saddle points of stable and nonstable multiplicities.

Planetary gear trains are, generally, dissipative dynamic systems operating in a complex dynamic process which produces different effects. These effects may occur in many various ways and may cause stochastic behaviour in the planetary gear train operation. Main generators of nonlinearity in case of planetary gear trains may be: rigidity characteristics of the teeth in a wheel, central wheel deformability, claw couplings and elements of the satellite assembly, dissipative forces within the gear train, defects in element construction, load distribution between the satellites, lubrication and *striking* processes in the planetary gear trains, etc. All these may be the cause of stochastic behaviour of a system.

In references [2-6,8] the dynamics of planetary gear trains has been studied. In this paper, for the adopted dynamic model exposed to disturbances characteristic for the dynamic process in the gravitational field, the configuration of dynamic equilibrium and the structure of the phase portrait have been studied. Based on the analytical solutions and numerical results, graphic presentations of nonlinear phenomena through surfaces of total system energy, portraits of constant energy curves and phase trajectories for different system parameters, have been given.

Information acquired from a fundamental monography [12] on nonlinear oscillations and a reference [11] about coupled singularities trigger, have been used.

In case of this dynamic model, special attention has been given to disturbances characteristic for dynamic processes in the gravitational field, so they may be the result of different factors such as: disturbancy forces mainly generated by the engagement of the teeth in a wheel, gear wheels and

[1)] Higher Technical-Technological School, F. Filipovi a 20, 17500 Vranje

claw couplings, dissipative forces, defects in element construction and assembling, irregular load distribution on the satellites. These disturbances are presented by additional masses of loose distribution and the dynamic model shown in Fig.1 has been formed, where 1-solar tooth wheel, 2-satellites, 3-epicycle and h-satellite bearing, and the disturbances have been presented by additional masses m_i.

Disturbance "masses" may take different positions depending on the disturbance we wish to analyse and assign significance to. Fig.1 shows the distribution of "masses" where m_1 represents a disturbance caused by irregular coupling of the solar tooth wheel with the satellite, m_2 represents a disturbance caused by defects in the solar tooth wheel-construction and assembling, masses m_3 and m_4 represent the mass disturbances caused by unequal load transfer, defects in construction and assembling the satellite, and mass m_5 represents a disturbance due to defective construction, unhomogeneity of the material, unprecise assembling of the satellite bearing and uneven load transfer from the satellite.

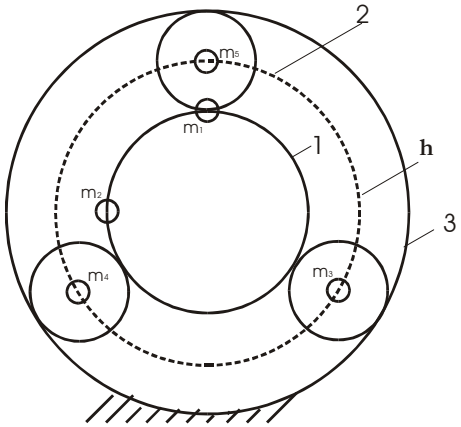

Dynamic model of the planetary gear train

The system potential energy according to the adopted dynamic model (Fig.1) is

$$E_p = m_1 g r_1 (1+\cos\varphi_1) + m_2 g r_1 (1+\sin\varphi_1) + m_{34} g r_h (2-\cos\varphi_h) + m_5 g r_h (1+\cos\varphi_h) \quad (1)$$

where m_3=m_4=m_{34}, r_1, r_h- divisional (basic) radiuses of the solar teeth wheel and the satellite bearing, φ_1 and φ_h- coordinates (the solar teeth wheel angles of rotation- 1 and the satellite bearing - h). For the generalized coordinate, φ_1 and φ_h are adopted.

If in the position of equilibrium the function of conservative holonomic scleronomic system force has its maximum (potential energy minimum), the equilibrium position of the system is stable, unstable or indifferent in all other cases. The Leyen-Dirichlet theorem has been used for the comparison, and the criterion of equilibrium and stability resulting from the facts stated above has the following form

$$\frac{\partial E_p}{\partial \varphi_i} = 0 \;\; ; \;\; \frac{\partial^2 E_p}{\partial \varphi^2} = \begin{cases} > 0 \text{ stable} \\ = 0 \text{ indifferent} \\ < 0 \text{ unstable} \end{cases}$$

In this case

$$\left.\frac{\partial E_p}{\partial \varphi_i}\right|_{\varphi=\varphi_i} = 0 \quad \text{for} \quad \varphi_1 = \frac{\pi}{4}, \frac{5}{4}\pi, \frac{9}{4}\pi,$$

$$\varphi_h = 0, \pi, 2\pi$$

Accordingly, the first deduction of potential energy equals zero in different positions and configurations. Table 1 gives characters of equilibrium positions for different mass positions.

Case	φ_1	φ_h	Condition	$\frac{\partial^2 E_p}{\partial \varphi_i^2}$	Character of the equilibrium position
I	1/4 π	0	$m_5 > m_{34}$	< 0	Unstable
			$m_{34} > m_5 + \sqrt{2}\,(m_1+m_2) r_1$	> 0	Stable
			$m_{34} = m_5 + \sqrt{2}\,(m_1+m_2) r_1$	$= 0$	Indifferent
II	1/4 π	π	$m_5 < m_{34}$	< 0	Unstable
			$m_5 > m_{34} + \sqrt{2}\,(m_1+m_2) r_1$	> 0	Stable
			$m_5 = m_{34} + \sqrt{2}\,(m_1+m_2) r_1$	$= 0$	Indifferent
			$m_5 = m_{34}$	< 0	Unstable
III	5/4 π	0	$m_5 < m_{34}$	>0	Stable
			$m_5 > m_{34} + \sqrt{2}\,(m_1+m_2) r_1$	> 0	Unstable
			$m_5 = m_{34} + \sqrt{2}\,(m_1+m_2) r_1$	$=0$	Indifferent
			$m_5 = m_{34}$	>0	Stable
IV	5/4 π	π	$m_5 > m_{34}$	>0	Stable
			$m_{34} > m_5 + \sqrt{2}\,(m_1+m_2) r_1$	< 0	Unstable
			$m_{34} = m_5 + \sqrt{2}\,(m_1+m_2) r_1$	$=0$	Indifferent

During nonlinear system stability testing, the first thing is to determine the conservative system equilibrium position, and then to examine the motion of the system around each equilibrium position. The change in the dynamic system parameter value may cause a change in the number of system equilibrium positions or their stability. Local motion of a system is characterized by some properties characteristic for linear systems and it is therefore justified to use minorization and linearization in such cases.

A conservative system is usually a rough approximation of real nonlinear systems, and it gives satisfactory results up to a certain point only [1]. The mechanical energy conservation law is an important characteristic of conservative systems.

For the conservative system of the defined planetary gear train model, the overall energy equals

$$E_k + E_p = h = E \quad (2)$$

where E_k- kinetic energy of the system, E- total energy of the system.

The kinetic energy of the studied model (Fig.1) is

$$E_k = \frac{1}{2}[I_1 \dot{\varphi}_1^2 + (m_1+m_2) r_1^2 \dot{\varphi}_1^2 + 3M_2 r_h^2 \dot{\varphi}_h^2 + (2m_{34}+m_5) r_h^2 \dot{\varphi}_h^2 + 3I_2 \dot{\varphi}_2^2] \quad (3)$$

where I_1, I_2- mass inertia axial moments of the solar teeth wheel and the satellite, r_1, r_h – basic radius of the solar teeth wheel and the satellite bearing, φ_1, φ_2, φ_h- angular velocities of the solar teeth wheel, satellite and satellite bearing.

Considering the wheel contact, the following relation between the angular velocities of the teeth wheels is deduced

$$\dot{\varphi}_2 = i_{21}^h \dot{\varphi}_1 + i_{2h}^1 \dot{\varphi}_h$$

where i_{jk} - transfer relations.

The transfer relations of the studied reductor model

wheel joints are 4.42. Taking into account the possibility of replacement, $\varphi_1=3.42\varphi_h$. These two replacements give the following form to the kinetic energy expression

$$E_k = \frac{1}{2}[11.696I_1 + 11.696(m_1+m_2)r_1^2 + \\ + 3M_2 r_h^2 + (2m_{34}+m_5)r_h^2 + 35.1I_2(\frac{r_1}{r_2})^2 + \\ + 3I_2(\frac{r_h}{r_2})^2 + 20.52I_2\frac{r_1 r_h}{r_2^2}]\dot{\varphi}_h^2 \quad (4)$$

For the planetary gear train kinetic parameters: m_1=0.5 kg, m_2=0.4 kg, m_{34}=0.1 kg, m_5=0.3 kg the total system energy expression was obtained

$$E = 0.2363\dot{\varphi}_h^2 + 0.198[1+\cos(3.42\varphi_h)] + \\ + 0.1584[1+\sin(3.42\varphi_h)] + 0.0855(2-\cos\varphi_h) + \\ + 0.2563(1+\cos\varphi_{h1}) \quad (5)$$

Q_k equals zero in the singular points. We can notice that the singular points of the integral curves appear in the points of the abscissa φ_h, where the potential energy has extreme values. Figs.2-4 confirm this for the given initial conditions. The mass perturbations are expressed in kilos (kg), (the unit will not be mentioned further on).

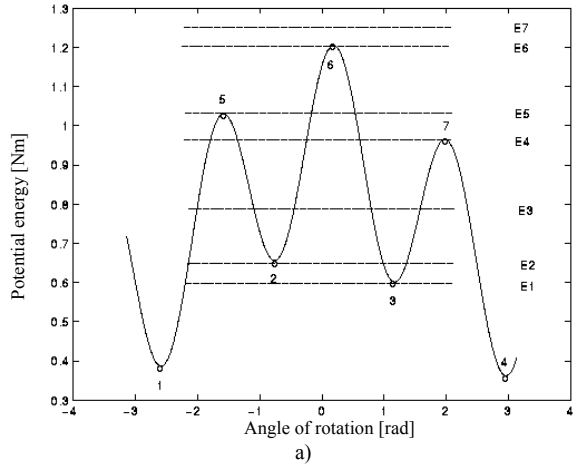

a)

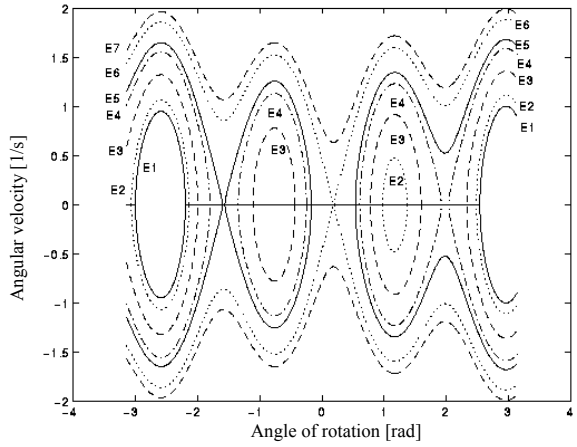

b)

a) potential energy curves and b) phase and constant energy curves for m_1=0.5, m_2=0.4, m_{34}=0.3 and for different initial conditions

Points 1-4 in Fig.2a represent the stable equilibrium positions. On the phase portrait or the portrait of constant energy curves (Fig.3, points 1-4) there are singular, central type points. Points 5-8 represent the unstable equilibrium positions and singular, unstable saddle points in the phase plane (Fig.3 points 5-8).

Fig.2b presents the phase trajectory and the constant energy curves E_i, as shown in Fig.2a. If the straight line E7, for the given initial conditions, is situated completely above the potential energy curve, the branches of the integral curve spread from infinity to infinity without cutting the abscissa in any point. The motion with the representative point moving along such curves from the initial position φ_0 and at the velocity φ_0 towards infinity, corresponds to the situation when the system revolves in one direction.

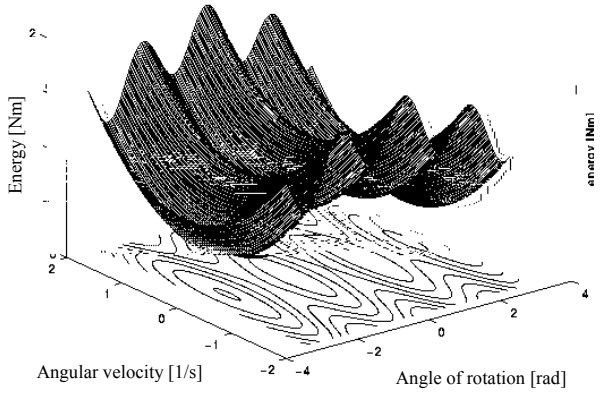

Constant energy curves family for the initial conditions as in Fig.2

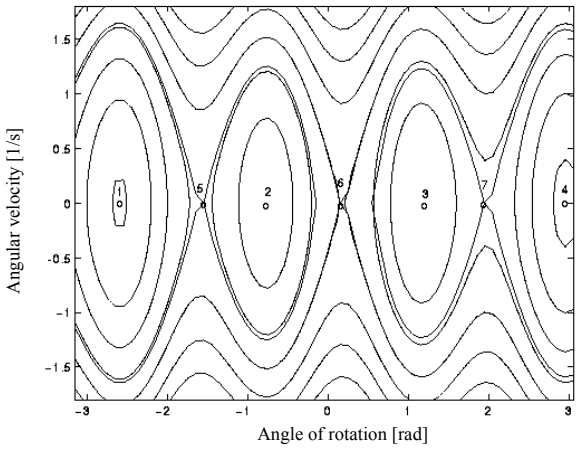

Graph of the system total energy surfaces for m_1=0.5, m_2=0.4, m_{34}=0.1 and m_5=0.3

When constant energy is given to a system in an initial moment, the chosen straight line E_i=const. intersects, makes the tangents at the maximum and minumum values (E6, E5, E2 and E1, Fig.2a) and cuts the potential energy curve at the bending point, which gives more than one phase curve isolated branches in the phase portrait, as shown in Fig.2b. For $E_p>E_i$ of φ, there are no trajectories in the phase plane. The phase trajectories exist for all the other values of φ where $E_p<E_i$, and they can be: closed curves Fig.2b (E1, E2, E3, E4), separatresses (E5, E6) and open branches E7. Separatresses are those phase trajectories which intersect each other in the saddle-type points (E5, E6, Fig.2b) and separate different kinds of curves. When the constant energy E_i given to the system in the initial moment grows, the obtained phase curves include the separatress and correspond to the periodic solutions. As the constant energy E_i decreases, the closed curves, included by the separatress, are obtained in the gives case.

The closed trajectories correspond to the periodic mo-

tion. Figs.5-8 present perturbation-deviation masses of the system, different from the case given above: m_1=0.5, m_2=0.2, m_{34}=0.1 and m_5=0.5.

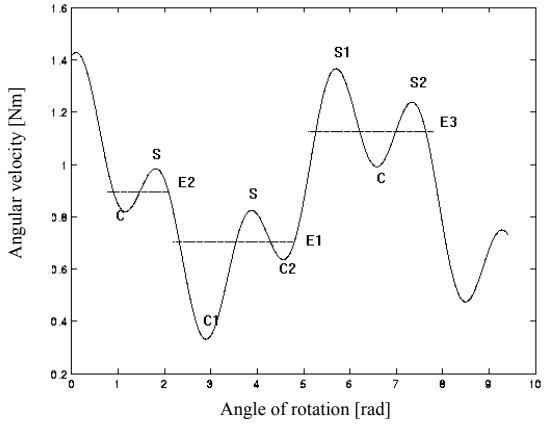

Potential energy graph m_1=0,5, m_2=0,2, m_{34}=0,1 and m_5=0,5

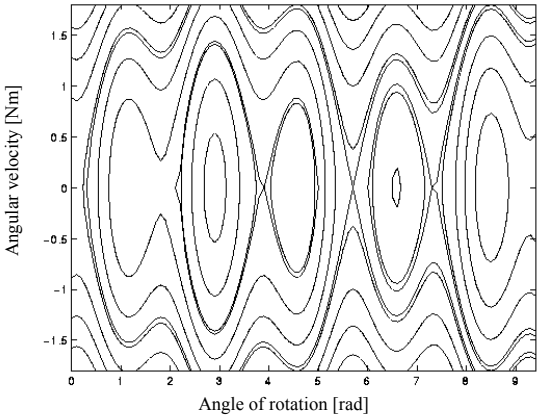

Constant energy curves family for a series of conditions as in Fig.5

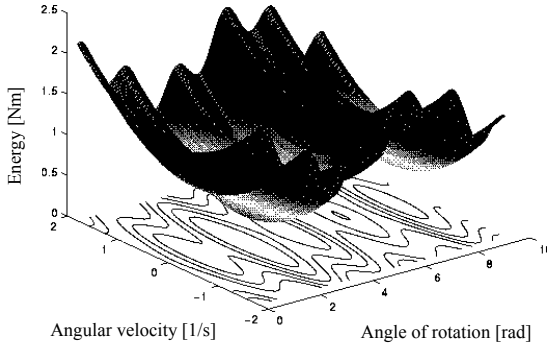

Graph of the total energy surface for m_1=0.5, m_2=0.2, m_{34}=0.1 and m_5=0.5

It is important to consider all the perturbance factors induced by eccentric masses deviative properties. There is however, quantitative difference from the previous case in the size of some masses, though the sum of the deviative masses stays the same. Should the graphs presenting the dependence of potential energy on the generalized coordinate, Figs.2 and 5, be compared, a difference between the curve shape and the number and type of extreme values will be noticed.

Fig.8 presents the phase trajectories in the phase plane for different values of the constant energy E_i (Fig.5) and different areas of the generalized coordinate.

The singular points of integral curves appear in the points with the abscissa φ where the potential energy has extreme values.

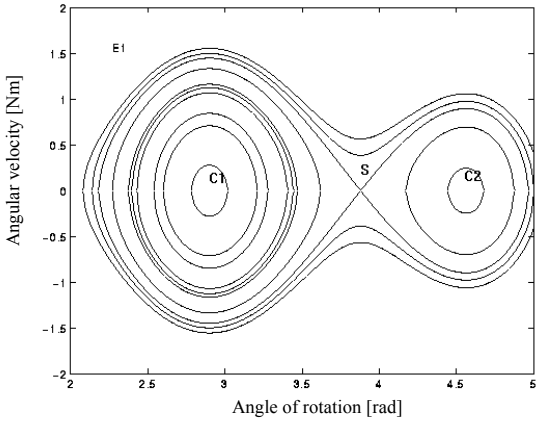

a)

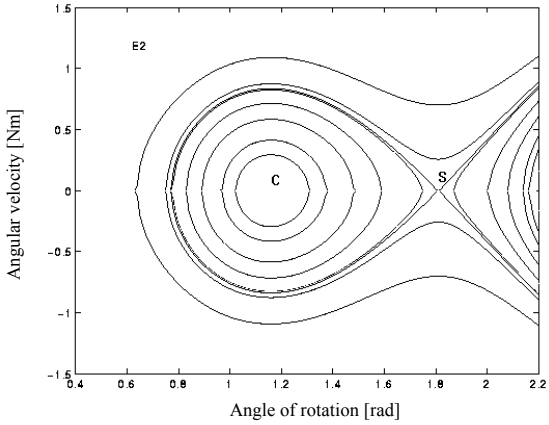

b)

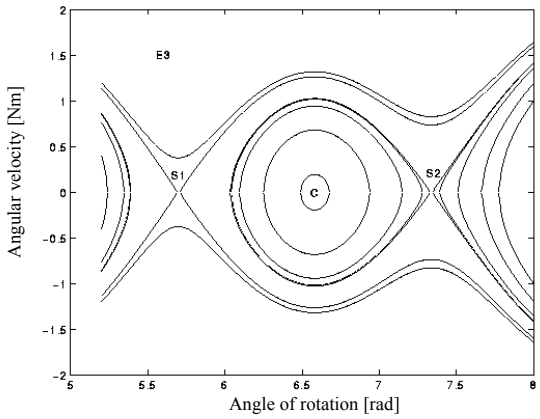

c)

Phase trajectories in the phase plane for different values of the constant energy: a) for the constant energy area E1 Fig.5 and the angle of rotation 2-5 [rad], b) for the constant energy area E2 Fig.5 and the angle of rotation 0.5-2.2 [rad], c) for the constant energy area E3 Fig.5 and the angle of rotation 5-8 [rad]

This can be confirmed by comparing two planes of the system dynamics state (φ, $E_p(\varphi)$) and (φ, $\dot{\varphi}$) with the same abscissa φ. Fig.8 presents integral curves and their singularities for different initial conditions and potential energy changes.

The potential energy has two local minimums and one

maximum in Fig.8a. Four branches of the integral curves pass through the singular saddle-type point S (homoclinic point), the abscissa of which corresponds to the potential energy maximum abscissa φ. This phase trajectory is called the separating line or the separatress because it is found where one trajectory shape transforms into another, separating trajectory branches of different shapes. Other trajectories do not intersect this point which corresponds to the unstable position of the system equilibrium in the phase plane. The energies E larger than the local maximum energies E_0, the phase trajectories consist of branches above the separatress. If $E<E_0$, the phase trajectories are closed branches rotating around the centre C1 or C2 and both of them, the motion corresponding to the periodic oscillations. This example confirms the existence of the trigger singularities which can be a cause of planetary gear train working unstableness.

Fig.8b shows the integral curves with saddle singularities, a closed and an opened branch. Fig.8c shows the integral curves with two saddles, two opened and a closed branch.

Figs.9 to 23 show the surfaces of the system total energy given by eq.(2) and the integral curves (phase trajectories) families in the phase plane and in the Descartes rectangular coordinate system (φ, $\dot{\varphi}$, E) for different system parameters, initial conditions and system total energy that induces motion.

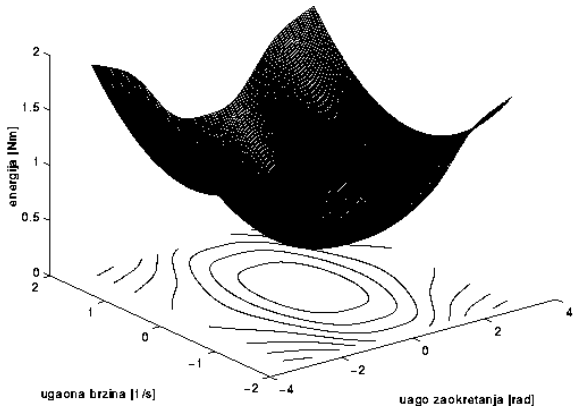

Graph of the surfaces of total energy for m_1

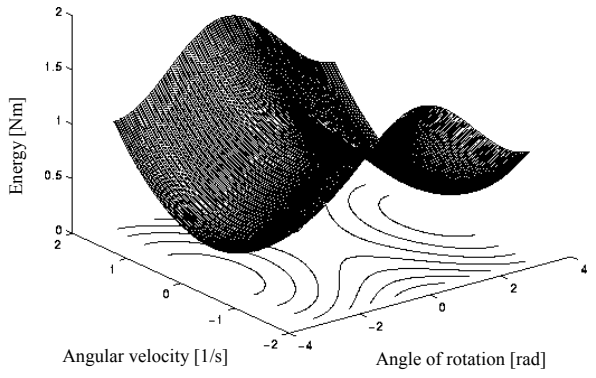

Graph of the surface of total energy for m_{34}=0.1 and m_5=0.5

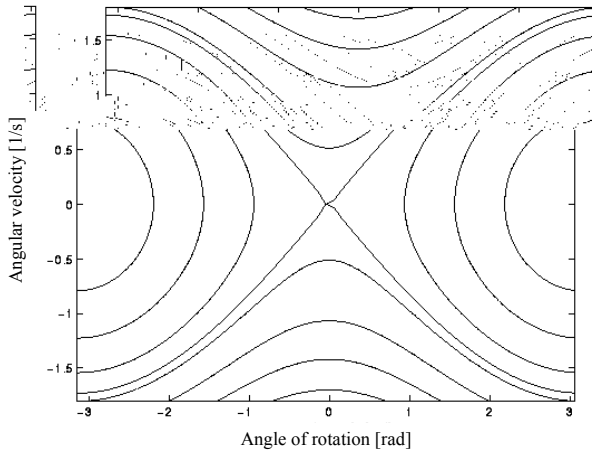

Constant energy curves family for the initial conditions as in Fig.15

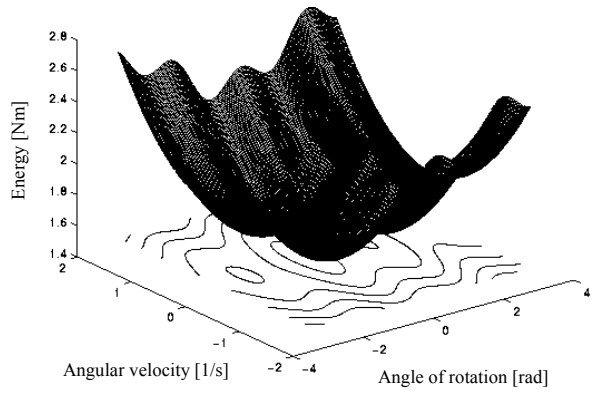

Graph of the surface of total energy for m_1=0.1, m_2=0.2, m_{34}=0.7, m_5=0.5

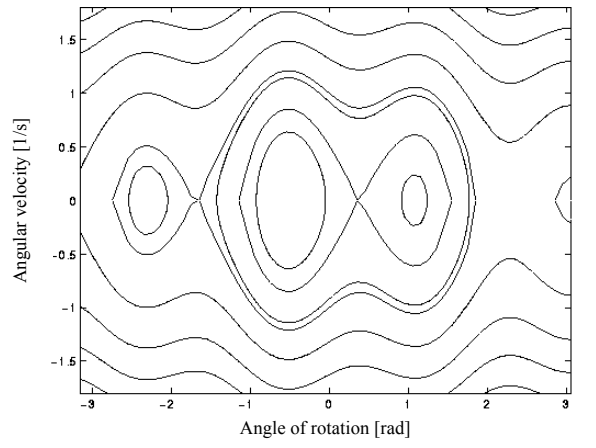

Constant energy curves family for the initial conditions as in Fig.17

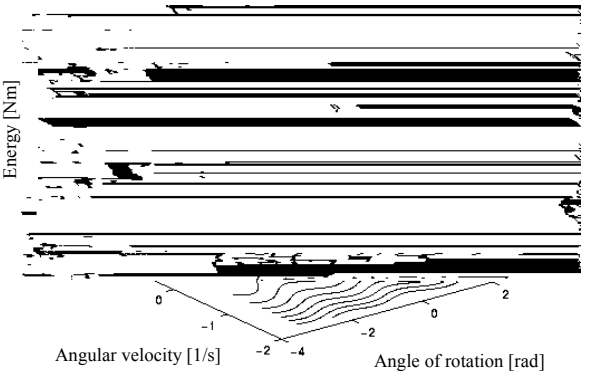

Graph of the surface of total energy for m_1=0.1, m_5=0.05

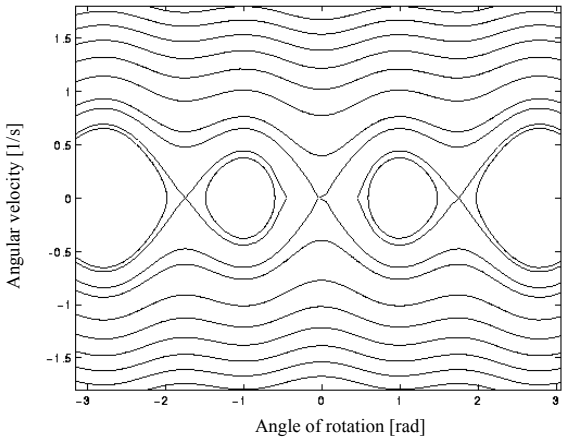

Constant energy curves family for the initial conditions as in Fig.19

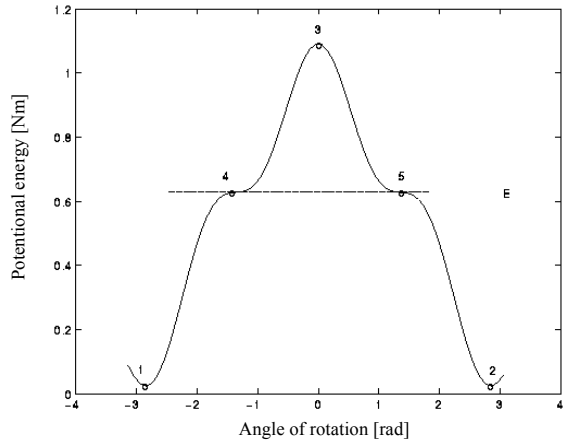

Graph of the surface of total energy for m_1=0.3 and m_5=0.5

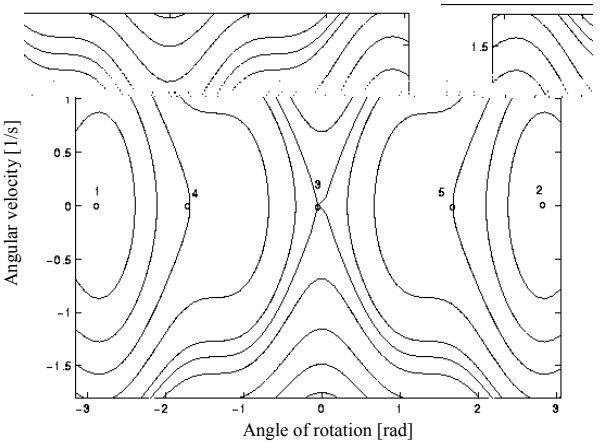

Constant energy curves family for the initial conditions as in Fig.21

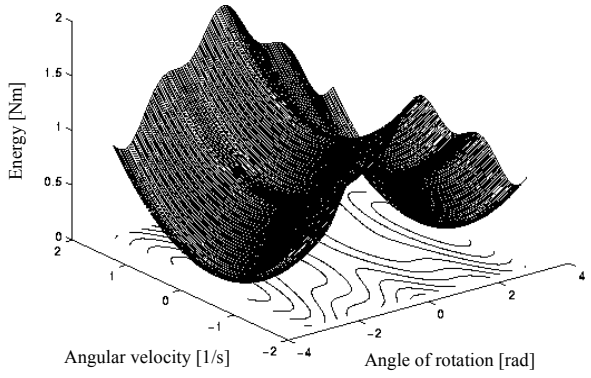

Graph of the surface of total energy and the portrait of constant energy curves for m_1=0.3 and m_3=0.5

During this, a significant change has occurred in the graph shape, potential energy, total energy surface and the family of constant energy curves portraits. In Fig.9 only one position, the position of stable equilibrium, is distinct, during discrete change of these parameters. In Fig.11, seven equilibrium positions can be noticed, three saddle singularities and three center type singularities. The change of parameter numbers and values produces a change of singularity numbers with distinct, eight-shaped separatresses (Figs.12, 18 and 20).

Points 1 and 2 in Fig.21 correspond to the stable equilibrium positions and are center-type points on the phase portrait (Fig.22, points 1,2), while point 3 corresponds to the unstable equilibrium position and is an unstable, saddle-type singular point in the phase plane (Fig.22, point 3). Points 4 and 5 also correspond to the unstable equilibrium position but are areas with the peak in the phase plane (Fig.22).

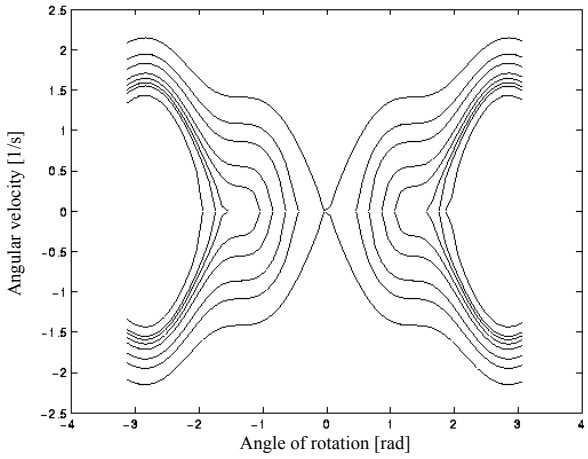

Integral curves in the phase plane

Fig.24. gives the integral curves corresponding to a particular area of constant energy (from 0.5 to max., Fig.21). For E_{max}, the integral curve consists of four branches, passing through the saddle-type point (see Fig.24). For $E_i<E$ (Fig.24) the phase trajectories are open branches left and right from the saddle-type point. When $E_i=E$ (constant energy presented by E line in Fig.24) the integral curves in the phase plane are curves with the peak on the abscissa, corresponding to the bending point, with the unstable equilibrium position (see Fig.24).

Figs.2-24 show that the potential energy function E_0 has the minimum integral curve passing into the singular point--center. When $E>E_0$ the closed integral curves surround the singular center-type point. These singular points are stable centers, since potential energy is at the minimum (Fig.2, Fig.8, etc.) judging from the above given Lagrange theorem. Slight disturbances around those positions give periodic movement.

For the maximum E, the integral curves have four branches, passing through the saddle-type singular point, with the abscissa corresponding to the generalized maximum potential energy coordinate abscissa (this is shown in all the constant energy curves graphs). What we have in this case is: asymptotic movement towards the homoclinic unstable equilibrium position or aperiodic unstable movement.

When the potential energy function has a bending point, the first and the second derivative equal zero, i.e. when the tangent to the energy curve at that point is horizontal, as the integral curve in the phase plane, a curve with the peak appears on the abscissa, which corresponds to the bending point. This is depicted in Figs.22 and 24 and the equilibrium position that points 4 and 5 correspond to is unstable.

The analysis of graphs 2-24 imposes the following conclusions.

At discrete change in the values of dynamic systems mass disturbances the number of equilibrium positions and configurations and their stability also changes. This change of the structure and character of the nonlinear system equilibrium, due to the change in system parameters, is the subject of the bifurcation theory. Such parameter significations, where movement quality and typology characteristics are changing, are called critical or bifurcatic meanings.

With a discrete change of the values of the disturbance parameters of the masses m_i, the singular representative point corresponding to the system stability (Fig.9), loses its balance and disintegrates into three points, one saddle [12] and in its vicinity two singular center-type points as, new stable equilibrium positions appear as well as a new eight--shaped separatress (see Ref [11], (Figs.13,15,22)), or should we consider the change of the same parameters, the number of equilibrium positions disintegrates from three (Fig.18) into six centers and five saddles, i.e. a number of triggers of singularities appear. Through the analysis of the graphs it was observed that with a discrete change of mass parameters, both numerically and in quantity, the centers lose their stability and the triggers of singularities are formed (see Ref. [7]).

The potential energy curves with two isolated points and the change of their position can be noticed with different parameter meanings (Figs.2,4,6,12,18,20). For different parameters, the phase curves with a "peak" in which the equilibrium position is unstable appear (Figs.22 or 24). Less distinct "peaks" are in Figs.14 and 18 where unstable equilibrium positions may occur.

To enable small oscillations around the equilibrium position and to make presumptions about small oscillations valid, it is necessary that the potential energy has its minimum even in the equilibrium position, which is a condition for that position to be a stable equilibrium position.

According to the "deviation disturbances" positions as given in Table 1, it is obvious that besides the stable equilibrium positions, unstable and indifferent positions also exist. This does not depend only on planetary gear train "mass disturbances" position, but on particular parameter values as well (Table 1). The initial conditions determine whether the movement is periodic or aperiodic, and the very character of the phase trajectory.

This concept about the character of the characteristic nonlinear dynamics of the planetary gear train model, enables the continuation of research of the real planetary gear train dynamics under working conditions when it compulsively rotates under the effects of compulsive coupling driving source.

Uneven operations such systems in real working regime and noise are due to the existence of system characteristic nonlinearities.

We take this opportunity to thank the manager of this project, Prof. Katica Stevanovi -Hedrih, PhD for her useful suggestions and consulting regarding the formulation of this work. The research presented here is a part of Ministry of Science, Technology and Development of the Republic of Serbia projects, N^{0}1616 (Real problems in mechanics) and N^{0}1828 (Active structure dynamics and control).

[1] MOON,C.M., (1987), *Chaotic Vibrations,* An Introduction for Applied Scientists and Engineers, John Wiley & Sons, New York, 309 (Mun, F., , Mir, Moskva, p.305 (in Russian)).

[2] HEDRIH (STEVANOVI),K., KNEŽEVI ,R. Prilog izu avanju dinamike planetarnih prenosnika, *Naučnotehnički pregled*, 1998, vol.XLVIII, no.6, pp.26-36.

[3] HEDRIH (STEVANOVI),K., KNEŽEVI ,R. Analiza stabilnosti planetarnog prenosnika, *Naučnotehnički pregled*, 1999, vol.XLIX, no.2, pp.29-36.

[4] HEDRIH-STEVANOVI ,K., CVETKOVI ,S., KNEŽEVI ,R. Estimation of planetary reductor sensitivity. *Facta Universitatis, Series Mechanical Engineering*, University of Niš, 1999, vol.1, no.6, pp.683-694.

[5] HEDRIH-STEVANOVI ,K., CVETKOVI ,S., KNEŽEVI ,R. Planetarni prenosnik u turbulentnom prigušenju, *Naučnotehnički pregled*, 2000, vol.XLX, no.3, pp.46-50.

[6] KNEŽEVI ,R. *Nelinearni fenomeni u dinamici planetarnih prenosnika.* doktorska disertacija, Mašinski fakultet, Niš, 2001, p.177.

[7] HEDRIH-STEVANOVI ,K. *Izabrana poglavlja iz teorije nelinearnih oscilacija.* Mašinski fakultet, Niš, 1977 (1975), p.180.

[8] HEDRIH-STEVANOVI ,K., KNEŽEVI ,R., CVETKOVI ,S. Dynamics of Planetary Reductor with Turbulent Damping. *International Journal Nonlinear Sciences ond Numerical Simulation,* 2001, vol.2, no.3, pp.265-275.

[9] HEDRIH-STEVANOVI ,K.(1998), *Vectorial Method of the Kinetic Parameters Analysis of the Rotor with Many Axes and Nonlinear Dynamics,* Parallel General Lecture, Proceedings of the 3rd International Conference on Nonlinear Mechanics, Shanghai, 1998, pp.42-47.

[10] HEDRIH-STEVANOVI ,K. Nonlinear dynamics of a rotor with a vibrating axis, and sensitive dependence on the initial conditions of the forced vibration of a heavy rotor. *International Journal Nonlinear Oscillations,* 2000, vol.3, no.1, pp.129-145.

[11] HEDRIH-STEVANOVI ,K. *Trigger of coupled singularities.* 6th Conference on Dynamical Systems-Theory and Applications, Editors,J. Awrejcewicz and all., Lodz, 2001, pp.51-78 (Plenary Lecture).

[12] GUCKENHEIMER,J., HOLMES,PH., (1983), *Nonlinear Oscillations, Dynamical Systems, and Bifurcations of Fields,* Springer-Verlag, p.461.

Received: 10.10.2002

č

č č č č

č č

č č

č č

č č č ć

č

Ključne reči:

č č

l’

l’

l’ l’

l’

l’ l’ d’

l’ d’

Mots-clès: l’ d’ l’